JOURNAL OF GUIDANCE, CONTROL, AND DYNAMICS
Vol. 22, No. 1, January–February 1999

Evaluation of the Naval Space Surveillance Fence Performance Using Satellite Laser Ranging

G. Charmaine Gilbreath*
U.S. Naval Research Laboratory, Washington, D.C. 20375-5354
Paul W. Schumacher Jr.†
U.S. Naval Space Command, Dahlgren, Virginia 22448
Mark A. Davis‡
AlliedSignal Aerospace Company, Lanham, Maryland 20706
Edward D. Lydick§
U.S. Naval Space Command, Dahlgren, Virginia 22448
and
John M. Anderson¶
U.S. Air Force Research Laboratory, Albuquerque, New Mexico 87177

An experiment is described in which the performance of the Naval Space Command Fence Receiver Suite is evaluated using satellite laser ranging. Fence measurement accuracy and precision is presently assessed based on cataloged orbits, which are not sufficiently accurate for rigorous calibration and trend identification. Satellite laser ranging is a well-known high-precision data type, which can provide submeter reference positions routinely. Two methods of sensor evaluation are investigated. One is an ephemeris-based approach, where a truth reference orbit is determined from laser ranging data from a number of different satellites at different altitudes. Fence-based residuals are then computed from this truth. The second is a geometric method, which computes satellite positions directly using ranging data and angle data from the telescope. A mathematical treatment of the geometric dilution of precision for both methods is included in the discussion. The overall experiment showed that the fence sensor suite is operating to within 14–17 times its noise floor of 10 μrad at zenith. We believe that this is the most extensive measurement of the fence performance utilizing an external and independent data type, and due to the precision of the data type, its overall response and error trends are identified.

I. Introduction

THIS paper describes an experiment conducted with the Naval Space Command fence and the Naval Research Laboratory's satellite laser ranging (SLR) system integrated on the 3.5-m telescope at the U.S. Air Force Research Laboratory Starfire Optical Range (NRL@SOR). The current assessment of fence measurement accuracy and precision is based on cataloged orbits. However, these orbits are not sufficiently accurate for rigorous data calibration. SLR-derived reference positions can provide the required accuracy. The purpose of the experiment was to demonstrate the feasibility of using laser radar for independent external performance evaluation of the sensor receivers. Two methodologies were investigated. Both methods proved viable, and each method appears appropriate for operational calibration within a specific regime.

Precision ephemerides for known objects were derived using SLR data from NRL@SOR as well as from other SLR sites located globally. Positions were then interpolated from the ephemeris at the times of the crossing of the fence and at Elephant Butte, in particular. This method of calibration was compared to a geometric method, where position was derived directly from SLR and angle data that were obtained simultaneously with fence crossings. Such a comparison of techniques was made possible by the proximity of NRL@SOR to the Elephant Butte receiver site.

Results presented show the extent to which the fence performance can be evaluated and calibrated using truth ephemeris and postprocessing, as well as in real time using simultaneous range and angle data from an SLR site nearly collocated with a fence receiver. To our knowledge, these are the first such data presented on this subject for the fence, and the first comprehensive insight is provided into error trends in the receiver system because of the higher precision and accuracy of the SLR-derived reference data.

II. Fence

The Naval Space Surveillance sensor system (NAVSPASUR fence) operated by Naval Space Command (NAVSPACECOM) is a continuous-wave multistatic radar deployed across the southern United States along a great-circle arc, which defines an east–west baseline for the rf interferometer. This system has come to be known as the fence. Figure 1 shows the facilities located across the United States. The fence provides real-time unalerted detection and metric observations for a majority of the near-Earth space object population and many high-altitude objects. The fence detects essentially all trackable near-Earth satellites having orbital inclinations of 30 deg or greater. It records about 160,000 observations daily and forward up to 22,000 triangulated satellite positions to the Space Control Center (SCC) in Cheyenne Mountain. The yield provides data on a majority of objects in the total space catalog.

The sensor suite consists of three transmitters and six receivers located across the southern United States. The fence measures direction cosines giving the apparent angular position of space objects with respect to the receivers. The basic geometry is shown in Fig. 2, where the cosine is defined in terms of the baseline orientation of the antennas. The definition of the direction cosines is

$$\cos\theta = \hat{\boldsymbol{s}} \cdot (\boldsymbol{b}/b) = p/b \tag{1}$$

$$\cos\theta = \phi(\lambda/b) \tag{2}$$

where $\hat{\boldsymbol{s}}$ is the unit vector in the direction of the satellite, $b = |\boldsymbol{b}|$, p is the path length difference from the source to the two antennas,

Received Oct. 16, 1997; revision received June 8, 1998; accepted for publication June 8, 1998. This paper is declared a work of the U.S. Government and is not subject to copyright protection in the United States.

*Head, Electro-Optics Technology Section, Code 8123. Member AIAA.
†Technical Advisor, Aerospace Engineer, Analysis and Software Branch, Information Systems Division, 5280 Fourth Street. Member AIAA.
‡Project Engineer, Earth Sciences and Laser Technologies, 7515 Mission Drive.
§Physicist, Analysis and Software Branch, Information Systems Division, 5280 Fourth Street.
¶Lt. Colonel, Starfire Optical Range, LIG, 3550 Aberdeen Avenue SE.

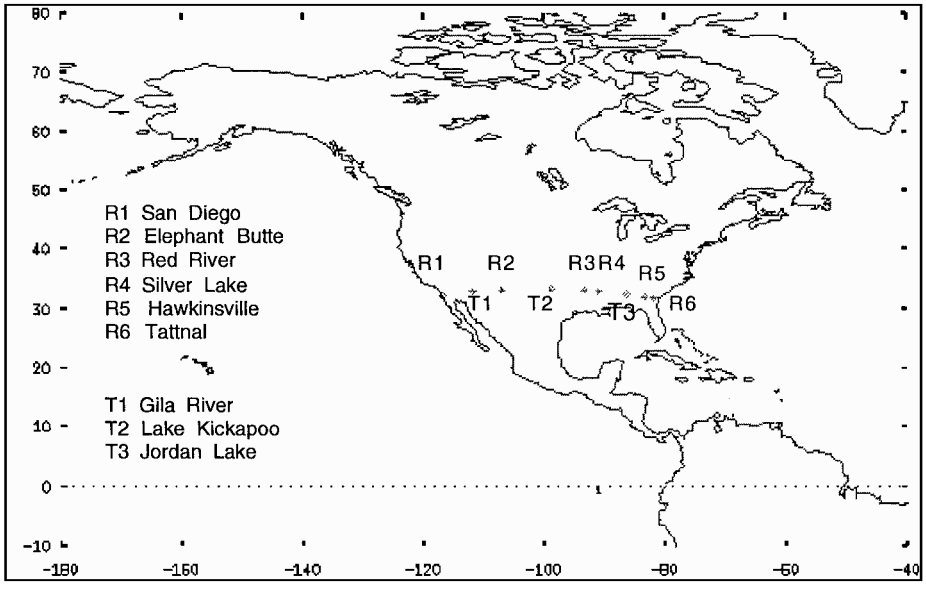

Fig. 1 Map of the facilities.

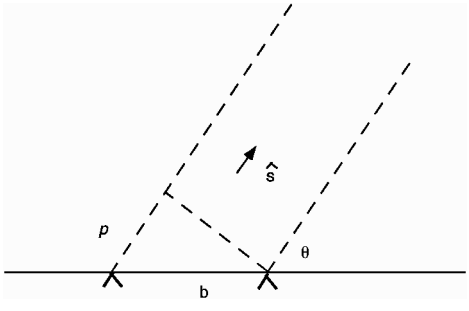

Fig. 2 Geometric description of cosine θ as constrained by the interferometer's baseline and orientation of antennas.

and ϕ is the measured phase. The error in direction cosine resulting from the phase measurement error is

$$d\cos\theta = d\phi(\lambda/b) \tag{3}$$

where $2\pi\phi = 2\pi p/\lambda$. Each site contains baselines from 9 to 557 m through the combination of various antenna elements.

The main transmitter radiates at the single frequency of 216.980 MHz, whereas the two auxiliary transmitters radiate at 216.970 and 216.990 MHz, respectively. The receivers are designed to detect signals that are Doppler shifted by up to 15 kHz from the center frequency. By design, the transmitter and receiver beams are confined near an Earth-fixed great-circle plane inclined at about 33 deg to the equator, forming a radar fence. The station locations span a 35-deg arc of longitude between 117° and 82° west. Coverage of satellite passes between these limits is assured for near-Earth orbits having inclinations above 33 deg. Over the Atlantic and Pacific Oceans, coverage is altitude dependent because of horizon limitations, but does extend to orbits of lower inclination. Though its strength is in detection of near-Earth satellites, the system routinely makes detections at slant ranges of more than 25,000 km and occasionally at ranges of more than 40,000 km, giving it wide coverage in both altitude and longitude.

The primary system observables of these interferometers are values of east–west (EW) and north–south (NS) direction cosines measured nearly simultaneously at each of the six receiver stations. The system accuracy is among the best for high-volume space surveillance sensors. Specifically, the precision of EW cosine residuals, reckoned over the entire catalog, is about 0.000200 rms, and it is known that orbit model errors contribute substantially to these residuals. Additionally, the system produces estimates of Doppler shift, Doppler rate, and cosine rates as byproducts of the primary data reduction.

The cosine data can be triangulated, producing estimated position values, and for practical operational reasons, this is done when NAVSPACECOM reports observations to the SCC. However, for updating the orbital elements, it is better to use the angles-only data themselves. The direction-cosine data are available at NAVSPACECOM, where they are used for Alternate Space Control Center (ASCC) catalog maintenance, whereas the SCC uses the triangulated positions in an azimuth-elevation-range format that is compatible with data from other radars in the space surveillance network.

III. SLR

SLR is a well-known technique, which can provide independent positions to centimeters for objects whose surface geometries are well known and for which orbits are well sampled. SLR uses direct detection in the optical regime to time tag the two-way range to a given satellite. This value is then corrected for system errors and combined with range data from other sites. The ensemble of data is then reduced and analyzed using orbit determination models. It has been demonstrated that NASA's GEODYN, a batch least-squares method, can produce position estimates accurate to centimeters[1] when the orbit is optimally sampled. Figure 3 shows the technique. In Fig. 3a, a time-tagged two-way range is obtained using incoherent optical radar, where R is range, $\Delta\tau_c$ is the roundtrip corrected time of flight, and c is the speed of light. In Fig. 3b, the range is corrected for system delays and analyzed using orbit determination modeling to finally produce a spacecraft's ephemeris.

In March 1995, first returns were obtained from a new experimental high-precision SLR station for the Department of Defense. NRL integrated a 300-mJ, 250-ps, 10-Hz, doubled-Nd:YAG system on the 3.5-m telescope at NRL@SOR.[2] This ranging capability was operational from March 1995 to March 1997. This capability presented an extremely robust link. The energy-area figure of merit for NRL@SOR is 2.88, which is 65 times greater than the NASA 0.75-m ground systems. Precision to LAGEOS, a satellite used by the international community for geoscience and calibration, from NRL@SOR was on the order of 2–3 mm one sigma, and accuracy was on the order of 1 cm, one sigma.

This powerful capability provided data for precision orbit estimation for spacecraft spanning ranges from 400 to 40,000 km using retro-enhanced satellites. Specifically, returns from spacecraft as high as 22,000 km have been routinely obtained from NRL@SOR. Tracking and acquisition agility has been demonstrated against spacecraft as low as 380 km, enabling successful ranging to the German satellite GFZ.

NRL@SOR is located 175 km to the north of Elephant Butte, where one of the fence's most sensitive receivers is located. This circumstance allows calibration using SLR measurements that are

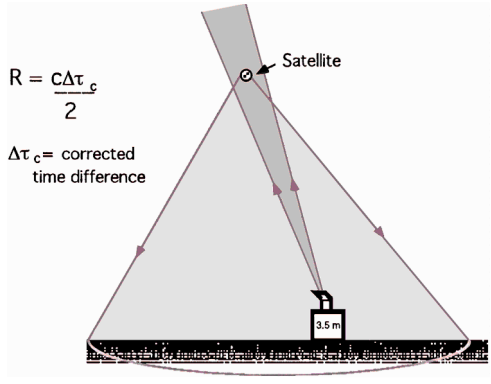

a) Range obtained

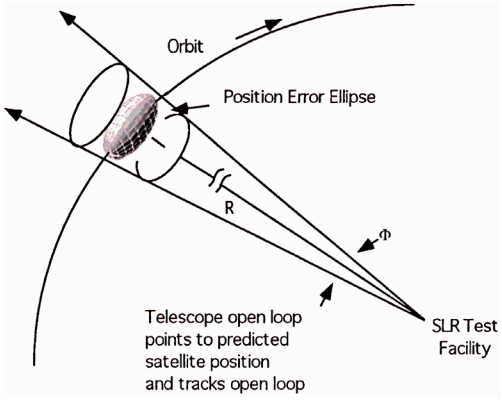

b) Position determination

Fig. 3 SLR.

simultaneous with fence crossings of satellites throughout a large range of altitudes. The proximity of these sites enabled the collection of a unique data set. These data provided the basis of analysis to determine if collocation of an SLR ground station with a fence receiver could provide a real-time method of calibration.

IV. Calibration Issues

Currently, the cataloged element sets may be in error by kilometers because of the simplified orbit models used to update the catalog in real time. Reckoned against the whole catalog, the cosine residuals usually fall in the neighborhood of 0.000200 rms, with biases almost an order of magnitude smaller. However, because the fence is a major contributor to the total observation base for the space catalog, the catalog residuals cannot form the basis for metric calibration. A rigorous calibration technique should use an independent data type that is at least an order of magnitude more accurate and precise than the fence measurements.

A type of internal calibration is routinely performed at the fence receiver stations. Every 30 min, a locally generated reference signal is injected into the receiver electronics downstream of the antennas themselves but ahead of the signal processing electronics. The signal simulates the antenna phases for a zenith pass of a satellite. By processing this calibration signal through the receiver electronics and interferometric algorithms, cosine variances can be derived that reflect the error contributions from these sources. Typically, these internal calibration cosine variances are about 0.000010, a value that approximates the noise floor of the current fence equipment, aside from possible systematic errors. The disparity between this internal calibration value and the quoted nominal value of 0.000200 rms represents the orbit model prediction error and the measurement errors due to space environmental effects along the propagation path, as well as antenna and cable physical variations. The critical question becomes: Is there an independent external means to gain insight into fence cosine measurement accuracy and precision in the region between 0.000200 and 0.000010?

It is well known that reference orbits can be determined to an accuracy of centimeters for selected satellites when sufficient SLR observations are available. The internal fence cosine variance is equivalent to about 10 μrad overhead, which is about 10 m of position at a range of 1000 km. Clearly, reference orbits accurate to less than 10 m at 1000 km can be used to assess both systematic and random errors in the fence measurements.

A. Geometric Dilution of Precision

Simple estimates for the level of cosine precision that could be assessed by SLR-derived data can be developed in both the ephemeris case and the geometric case. Of the two methods, the ephemeris case is simpler to analyze and will be considered first.

B. Ephemeris Method

The geometrical relation between ephemeris position $\boldsymbol{r}_{\text{eph}}$ and direction cosines measured at the same time (corrected for light time) is

$$\boldsymbol{r}_{\text{eph}} = \boldsymbol{R}_s + \boldsymbol{u}_s \rho_s \tag{4}$$

where $\boldsymbol{R}_s$ is the fence station position vector, $\boldsymbol{u}_s$ is the measured line-of-sight unit vector, and ρ_s is the slant range from the fence station. Figure 4 shows the sighting geometry.

The local topocentric frame at the fence station is defined by an orthonormal vector basis $(\boldsymbol{H}_s, \boldsymbol{E}_s, \boldsymbol{N}_s)$ representing the geodetic vertical, east and north directions, with respect to the great circle, rather than the true geographical directions. In particular,

$$\boldsymbol{u}_s = \sqrt{1 - m^2 - n^2}\boldsymbol{H}_s + m\boldsymbol{E}_s + n\boldsymbol{N}_s \tag{5}$$

where m is the EW direction cosine and n is the NS direction cosine. Consequently, on rearrangement of Eq. (4)

$$\boldsymbol{u}_s = (1/\rho_s)(\boldsymbol{r}_{\text{eph}} - \boldsymbol{R}_s) \tag{6}$$

and the components of interest are simply

$$m = (1/\rho_s)\boldsymbol{E}_s \cdot (\boldsymbol{r}_{\text{eph}} - \boldsymbol{R}_s) \tag{7}$$

and

$$n = (1/\rho_s)\boldsymbol{N}_s \cdot (\boldsymbol{r}_{\text{eph}} - \boldsymbol{R}_s) \tag{8}$$

Variations of m and n with respect to variations in ephemeris and station positions provide the basis for an approximate error analysis. Assume that all variations on the right-hand side are independent so that their net effect is described by a quadratic sum. Moreover, each squared variation can be interpreted as the variance (squared standard deviation) of the quantity. Then the EW cosine variance is

$$\begin{aligned}(\delta m)^2 = {} & \left(1/\rho_s^2\right)\left[(E_{sx})^2(\delta x_{\text{eph}})^2 + (E_{sy})^2(\delta y_{\text{eph}})^2\right. \\ & \left. + (E_{sz})^2(\delta z_{\text{eph}})^2\right] + \left(1/\rho_s^2\right)\left[(-E_{sx})^2(\delta X_s)^2\right. \\ & \left. + (-E_{sy})^2(\delta Y_s)^2 + (-E_{sz})^2(\delta Z_s)^2\right]\end{aligned} \tag{9}$$

where X, Y, and Z are the components of station position and x, y, and z are the components of ephemeris position. This approximate formula neglects implicit variations in the local basis vectors and the slant range, but otherwise gives the uncertainty in EW direction cosine due to given uncertainties in the ephemeris and station positions. This value is, therefore, the smallest measurement error that can be resolved using the given data. Finding all of the individual variances on the right-hand side calls for extensive analysis, beyond the scope of this discussion. But assigning the same value to each component of ephemeris uncertainty and likewise for the components of station position uncertainty yields a conservative upper bound. In that case, because $\boldsymbol{E}_s$ has unit magnitude,

$$(\delta m)^2 = \left(1/\rho_s^2\right)\left[(\delta \boldsymbol{r}_{\text{eph}})^2 + (\delta \boldsymbol{R}_s)^2\right] \tag{10}$$

As can be seen, the ephemeris errors and station position errors affect the limiting resolvable cosine error in the same manner. In practice, the surveyed station locations are uncertain at about the 1–2 m level, whereas the best SLR-derived ephemerides are uncertain at about the 0.1-m level. Therefore, at a typical slant range of 1000 km, cosine errors can be resolved at the level of 10^{-6}, well below the noise floor

of 10^{-5} quoted earlier for the present fence system. [Following the same reasoning, Eq. (10) also serves as the upper bound for the NS cosine variance.]

C. Geometric Method

As an alternate approach, it is of interest to know the level to which cosine precision can be assessed with a geometric solution using SLR data. That is, cosine uncertainties would be generated using SLR range and angle data only. No ephemeris would be generated. This approach would obviate the necessity of generating a reference orbit and might enable real-time response.

It is more complicated to estimate the resolvable cosine error when simultaneous SLR data is used without a reference orbit being generated. The reason is that the SLR sighting geometry has a strong effect on the results. The basic relation between fence measurements and simultaneous SLR measurements is

$$\boldsymbol{R}_c + \boldsymbol{u}_c\rho_c = \boldsymbol{R}_s + \boldsymbol{u}_s\rho_s \tag{11}$$

where $\boldsymbol{R}_c$ is the SLR station position vector, $\boldsymbol{u}_c$ is the SLR line-of-sight unit vector, and ρ_c is the SLR slant range. In terms of local topocentric basis vectors, the SLR line of sight is described by

$$\boldsymbol{u}_c = (\sin\varepsilon)\boldsymbol{H}_c + (\cos\varepsilon\sin\psi)\boldsymbol{E}_c + (\cos\varepsilon\cos\psi)\boldsymbol{N}_c \tag{12}$$

where ε is the elevation angle and ψ is the azimuth angle measured by the SLR station. These basis vectors are oriented with the geodetic vertical and true geographic east and north. Then the fence measurement vector is

$$\boldsymbol{u}_s = (\rho_c/\rho_s)\boldsymbol{u}_c + (1/\rho_s)(\boldsymbol{R}_c - \boldsymbol{R}_s) \tag{13}$$

and the components of interest, the EW and NS direction cosines, can be expressed as

$$m = (\rho_c/\rho_s)[(\boldsymbol{E}_s\cdot\boldsymbol{H}_c)\sin\varepsilon + (\boldsymbol{E}_s\cdot\boldsymbol{E}_c)\cos\varepsilon\sin\psi + (\boldsymbol{E}_s\cdot\boldsymbol{N}_c)\cos\varepsilon\cos\psi] + (1/\rho_s)\boldsymbol{E}_s\cdot(\boldsymbol{R}_c - \boldsymbol{R}_s) \tag{14}$$

and

$$n = (\rho_c/\rho_s)[(\boldsymbol{N}_s\cdot\boldsymbol{H}_c)\sin\varepsilon + (\boldsymbol{N}_s\cdot\boldsymbol{E}_c)\cos\varepsilon\sin\psi + (\boldsymbol{N}_s\cdot\boldsymbol{N}_c)\cos\varepsilon\cos\psi] + (1/\rho_s)\boldsymbol{N}_s\cdot(\boldsymbol{R}_c - \boldsymbol{R}_s) \tag{15}$$

Now for an approximate error analysis, consider the variations of m and n with respect to variations in the SLR measurements ρ_c, ε, and ψ and with respect to variations in station positions $\boldsymbol{R}_c$ and $\boldsymbol{R}_s$. Again, neglect implicit variations in the basis vectors and slant range. The limiting cosine error that can be resolved with given errors in all of these parameters is approximately

$$\begin{aligned}(\delta m)^2 = {} & \left(1/\rho_s^2\right)[(\boldsymbol{E}_s\cdot\boldsymbol{H}_c)\sin\varepsilon + (\boldsymbol{E}_s\cdot\boldsymbol{E}_c)\cos\varepsilon\sin\psi \\ & + (\boldsymbol{E}_s\cdot\boldsymbol{N}_c)\cos\varepsilon\cos\psi]^2(\delta\rho_c)^2 + \left(\rho_c^2/\rho_s^2\right)[(\boldsymbol{E}_s\cdot\boldsymbol{H}_c)\cos\varepsilon \\ & - (\boldsymbol{E}_s\cdot\boldsymbol{E}_c)\sin\varepsilon\sin\psi - (\boldsymbol{E}_s\cdot\boldsymbol{N}_c)\sin\varepsilon\cos\psi]^2(\delta\varepsilon)^2 \\ & + \left(\rho_c^2/\rho_s^2\right)[0 + (\boldsymbol{E}_s\cdot\boldsymbol{E}_c)\cos\varepsilon\cos\psi - (\boldsymbol{E}_s\cdot\boldsymbol{N}_c)\cos\varepsilon\sin\psi]^2 \\ & \times(\delta\psi)^2 + \left(1/\rho_s^2\right)\left[(E_{sx})^2(\delta X_c)^2 + (E_{sy})^2(\delta Y_c)^2\right. \\ & \left. + (E_{sz})^2(\delta Z_c)^2\right] + \left(1/\rho_s^2\right)\left[(-E_{sx})^2(\delta X_s)^2 + (-E_{sy})^2(\delta Y_s)^2\right. \\ & \left. + (-E_{sz})^2(\delta Z_s)^2\right]\end{aligned} \tag{16}$$

An exactly analogous formula would appear for the limiting NS cosine error that can be resolved, in which $\boldsymbol{N}_s$ replaces $\boldsymbol{E}_s$. It is clear that the limiting cosine errors depend strongly on the geometric circumstances, such as the actual azimuth and elevation of the SLR sighting and the relative positions of the two stations. There seems to be no simplification or further approximation that applies accurately in all cases.

V. Results and Discussion

A total of 37 simultaneous NRL@SOR SLR and fence passes were obtained over the DOY 303–323, 1996, inclusive.[3] Data were taken for a number of satellites are given in Table 1.

For a given crossing, a number of fence receivers obtained data from multiple transmitters and Doppler regions. The number of crossings from each of the fence sites is listed in Table 2. As can be seen from Tables 1 and 2, there were only 11 simultaneous NRL@SOR and fence collections for TOPEX, which yielded 199 receiver collects. If the simultaneity requirement is dropped, there were 1528 fence observations of TOPEX over the data collection period. In all, 37 simultaneous cases were acquired for all satellites in the data set. Thus, over 20 days, the sample size varied considerably between the two methods.

Table 1 Spacecraft and the 37 simultaneous NRL@SOR/fence crossings from Oct. 29, 1996 to Nov. 18, 1996

Spacecraft	Sat. no.	Height, km	Inclin., deg	Eccen.	NRL@SOR/ fence crossings
TOPEX	22076	1,319	66.0	0.0006	11
LAGEOS I	08820	5,812	109.9	0.0045	8
LAGEOS II	22195	5,598	52.6	0.0139	10
GPS 35	22779	20,166	54.3	0.0013	8
GPS 36	23027	20,012	55.1	0.0067	0

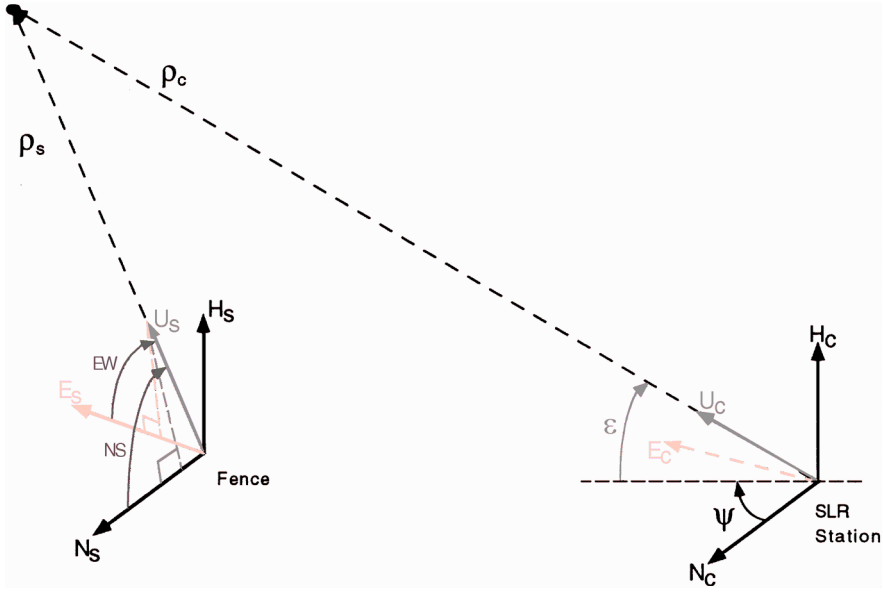

Fig. 4 Local topocentric vectors of the two sites and their relationship to the spacecraft in the instantaneous terrestrial frame.

Table 2 Fence measurements per site from Oct. 29, 1996 to Nov. 18, 1996

Spacecraft	Crossings	Measurements						Total fence collects
		San Diego	Elephant Butte	Red River	Silver Lake	Hawk-insville	Tattnal	
Ephemeris method								
TOPEX	119	258	252	256	272	236	254	1528
LAGEOS I	64	34	47	41	47	55	41	265
LAGEOS II	65	42	47	44	46	59	46	284
GPS 35	22	12	6	14	9	26	20	87
GPS 36	23	16	1	3	0	37	23	80
Geometric method								
TOPEX	11	42	33	28	36	29	31	199
LAGEOS I	8	8	8	7	8	7	6	44
LAGEOS II	10	10	9	10	11	10	9	59
GPS 35	8	5	3	4	3	10	7	32

Table 3 Ephemeris method cosine residuals computed from SLR ephemeris-based truth for all fence receivers: Oct. 29, 1996 to Nov. 18, 1996

Spacecraft	EW mean	EW std. dev.	NS mean	NS std. dev.	4σ Edit, %
TOPEX	0.000007	0.000167	0.000015	0.000206	3.3:50/1528
LAGEOS I	−0.000063	0.000148	−0.000032	0.000116	3.4:9/265
LAGEOS II	−0.000041	0.000152	−0.000022	0.000118	5.6:16/284
GPS 35	−0.000064	0.000169	−0.000052	0.000104	2.3:2/87
GPS 36	−0.000116	0.000180	−0.000059	0.000082	2.5:2/80
All	−0.000014	0.000167	−0.000001	0.000184	3.0:67/2244

Table 4 Geometric method cosine residuals computed from simultaneous NRL@SOR SLR and fence data for all fence receivers: Oct. 29, 1996 to Nov. 18, 1996

Spacecraft	EW mean	EW std. dev.	NS mean	NS std. dev.	4σ Edit, %
TOPEX	0.000030	0.000156	−0.000129	0.000184	3.5:7/199
LAGEOS I	−0.000033	0.000339	0.000056	0.000263	0.0:0/44
LAGEOS II	−0.000008	0.000147	−0.000049	0.000097	0.0:0/59
GPS 35	−0.000074	0.000181	−0.000039	0.000122	0.0:0/32
All	−0.000003	0.000161	−0.000083	0.000162	3.3:11/334

For this experiment, the SLR measurements were used in two different ways to produce a calibration reference for the fence data. As discussed in Sec. II, ephemeris solutions for the spacecraft listed were derived with GEODYN using data available from all SLR stations, including NRL@SOR. The positions were then found based on Hermite interpolation to times corresponding to the fence crossings. At the times of the fence crossings (light time corrected for the range to the fence receivers) the position was used to generate computed cosines for each fence site. The EW and NS fence data were the observed values used to create residuals.

For the geometric method, the SLR data taken at NRL@SOR simultaneously with the fence observations were compared directly with the fence data. Positions were estimated using experimentally measured range and angle data from NRL@SOR. These positions were used to generate cosines for comparison to the those observed by each fence receiver.

Tables 3 and 4 present the sample means and standard deviations of the EW and NS cosine residuals reckoned against both the ephemerides and geometric methods, respectively. In every case except one, the cosine precisions are better than the nominal 0.000200 figure from catalog-based statistics for EW after a recursive 4-sigma editing procedure eliminated spurious outliers. Also shown is the percentage and the number of measurements that are rejected.

The SLR determined ephemeris was computed from data available through NASA's Crustal Dynamics Data Information System (CDDIS)** for satellites that passed through the fence. The residuals were generated from these ephemerides. These results show that this approach can provide a very reliable and easily assessable means to characterize the performance of the fence sensor system. However, this is a post-processing methodology for independent calibration.

A comparison between Tables 3 and 4 indicates no obvious differences in precision using the simultaneous SLR/fence sensor technique, given uncertainties due to small sample size. The advantage of the latter procedure is that it is simple and fast, potentially lending itself to real time in field calibration.

Tables 5 and 6 present similar results receiver-by-receiver for a given satellite. Data for TOPEX have been selected as an example. The data set shows that the method can be a powerful, potentially real-time tool to assess error trends for a given sensor.

A consistent and interesting picture of fence performance emerges. The entire data set from this experiment represents the most extensive comparison done to date between actual fence data and high-precision external reference data. As such, these data indicate that the fence is performing better than measures based on cataloged orbits. Specifically, the fence sensor suite produces EW cosines having a precision of 14–33 times the noise floor (17 times the noise floor on average).

Because the SLR reference orbits are several orders of magnitude more accurate than the catalog orbits, the cosine accuracy assessment is inherently more reliable than that derived from the cataloged orbits.

There is no implication in the analysis and Tables 3–6 that collocating the SLR station with the fence station actually produces more accurate results. The complicated form of Eq. (16) suggests that a calibration effort based on simultaneous data would have to be carefully planned to extract the most accurate results. A further analytical treatment of the geometric method can be found in Ref. 4.

**Available at http://cddisa.gsfc.nasa.gov/.

Table 5 Ephemeris method cosine residuals per fence receiver for TOPEX, Oct. 29, 1996 to Nov. 18, 1996

Fence rcvr.	EW mean	EW std. dev.	NS mean	NS std. dev.	4σ Edit, %
San Diego	0.000084	0.000132	−0.000035	0.000190	3.8:10/258
Elephant Butte	−0.000035	0.000105	−0.000091	0.000185	5.6:14/252
Red River	0.000143	0.000129	0.000237	0.000175	1.2:3/256
Silver Lake	0.000060	0.000127	−0.000028	0.000170	0.7:2/272
Hawkinsville	−0.000255	0.000077	−0.000023	0.000183	6.4:15/236
Tattnal	0.000011	0.000084	0.000021	0.000157	2.4:6/254
All	0.000007	0.000167	0.000015	0.000206	3.3:50/1528

Table 6 Geometric method cosine residuals from simultaneous data per fence receiver for TOPEX, Oct. 29, 1996 to Nov. 18, 1996

Fence rcvr.	EW mean	EW std. dev.	NS mean	NS std. dev.	4σ Edit, %
San Diego	0.000098	0.000085	−0.000199	0.000138	0.0:0/42
Elephant Butte	−0.000023	0.000089	−0.000236	0.000213	6.1:2/33
Red River	0.000179	0.000099	0.000123	0.000076	3.6:1/28
Silver Lake	0.000109	0.000101	−0.000192	0.000109	0.0:0/36
Hawkinsville	−0.000260	0.000052	−0.000191	0.000125	10.3:3/29
Tattnal	0.000011	0.000067	−0.000020	0.000125	3.2:1/31
All	0.000030	0.000156	−0.000129	0.000184	3.5:7/199

Table 7 Difference in residual statistics from comparison of geometric with ephemeris methods

	All	TOPEX	LAGEOS1	LAGEOS2	GPS 35
			EW std. dev.		
Minimum	−0.0000046	−0.0000016	−0.0000082	−0.0000082	−0.0000130
Maximum	0.0000021	0.0000020	0.0000083	0.0000039	0.0000120
Average	0.0000001	0.0000004	−0.0000009	−0.0000013	−0.0000007
			EW mean		
Minimum	−0.0000033	−0.0000018	0.0000100	−0.0000013	−0.0000036
Maximum	0.0000041	0.0000016	0.0000217[a]	−0.0000089	0.0000190
Average	0.0000001	0.0000002	0.0000152	−0.0000117	0.0000007
			NS std. dev.		
Minimum	−0.0000119	−0.0000017	−0.0000126	−0.0000138	−0.0000250[a]
Maximum	0.0000105	0.0000004	0.0000077	−0.0000056	0.0000196
Average	−0.0000042	−0.0000011	−0.0000080	−0.0000044	0.0000075
			NS mean		
Minimum	0.0000005	0.0000074	−0.0000121	0.0000094	−0.0000223[a]
Maximum	0.0000156	0.0000148	0.0000044	0.0000132	−0.0000054
Average	0.0000077	0.0000118	−0.0000077	0.0000112	−0.0000115
			Sample size		
Geometric	323	192	45	59	32
Ephemeris	2177	1478	256	268	85

[a]Cases where the differences in the compared residuals exceeded sensor electronic noise floor by greater than a factor of 2.

A basic result of this experiment was that directly comparing fence data and SLR data is feasible in practice and that it can be done precisely enough to establish a useful external calibration of the fence data. The differences for the sensor suite residual statistics produced by the geometric and ephemeris methods are listed in Table 7. Based on the sample sets analyzed, the method-dependent error contribution exceeds the receiver electronics noise floor by a factor of 2–3. From Tables 3 and 4, it can be seen that the error component from the ephemeris method is consistently lower. However, the procedure to locate satellites using the geometric method is straightforward, although the error analysis is more complicated. Therefore real-time operational calibration becomes feasible. The geometric methodology does require simultaneously tasking the SLR calibrator to obtain data at specific fence crossing times and so mission planning becomes an added requirement for this method.

As the behavior of the individual components of the fence is being observed, it is important to examine the possible sources that might impact the accuracy of the comparison utilizing ephemeris points derived in the International Terrestrial Reference Frame system. The fence has been operating in the World Geodatic System 1972 coordinate system. The fundamental differences between these have been considered and found to be near the noise floor of the receivers in this case.

VI. Conclusions

An experiment has been described in which the performance of the NAVSPACECOM Fence Receiver Suite was evaluated using SLR, which is a data type known for its centimeter-level precision and accuracy. Two methods of sensor evaluation were investigated using this data type. The ephemeris method required postfit satellite position estimation derived from SLR data accessible in the international CDDIS data bank. The geometric method computed satellite position directly from laser ranging data and telescope angles. Residuals derived from both methods provided an assessment of sensor suite performance as well as insight into sensor-by-sensor biases. The fence as a suite was shown to be operating at 14–17 times its electronic noise floor of approximately 10 μrad on a zenith pass. A mathematical treatment of the geometric dilution of precision for both methods indicates that there can be a significant impact from pass geometries on the results, which pertain to the geometric

method in particular. A comparison of the results indicate that potential weights and biases derived from the standard deviations and means can provide a powerful tool to refine estimated postions of satellites detected by the fence.

In addition, the data from this experiment can help answer some important questions related to fence operations. For example, could the current fence data support more accurate cataloged orbit solutions if a more accurate orbit model were used? Can the residual statistics for cosines (or other fence observables) be used to diagnose equipment problems at individual stations? What is the error source causing a small percentage of the measurements to be rejected? To what extent should the calibrator and the fence sensor be collocated to obtain meaningful results? In-depth consideration of these questions is beyond the scope of this paper and is the subject of future work.

Acknowledgments

The authors would like to acknowledge the teams at U.S. Naval Research Laboratory and the U.S. Air Force Research Laboratory Starfire Optical Range for their dedicated efforts to collect the data that made this paper possible.

References

[1]Degnan, J. J., "Millimeter Accuracy Satellite Laser Ranging: A Review," *Contributions of Space Geodesy to Geodynamics: Technology*, Geodynamics Series, Vol. 25, American Geophysical Union, Washington, DC, 1993, pp. 133–162.

[2]Gilbreath, G. C., Davis, M. A., Rolsma, P., Eichinger, R., Meehan, T., and Anderson, J. M., "Naval Research Laboratory at Starfire Optical Range: Satellite Laser Ranging with Robust Links," *Laser Radar Technology and Applications II*: *Proceedings of the Society of Photo-Optical Instrumentation Engineers*, edited by G. W. Kamerman, Vol. 3065, Society of Photo-Optical Instrumentation Engineers, Bellingham, WA, 1997, pp. 116–130.

[3]Gilbreath, G. C., Schumacher, P. W., Jr., Davis, M. A., Lydick, E. D., and Anderson, J. M., "Calibrating the Naval Space Surveillance Fence Using Satellite Laser Ranging Data," *Proceedings of the 1997 AAS/AIAA Astrodynamics Specialist Conference*, Univelt, San Diego, CA, 1997, pp. 403–416; also American Astronautical Society Paper 97-625, Aug. 1997.

[4]Schumacher, P. W., Jr., Gilbreath, G. C., Lydick, E. D., and Davis, M. A., "Error Analysis for Laser Based Metric Calibration of the Naval Space Surveillance System," *Laser Radar Technology and Applications III*: *Proceedings of the Society of Photo-Optical Instrumentation Engineers*, edited by G. W. Kamerman, Vol. 3380, Society of Photo-Optical Instrumentation Engineers, Bellingham, WA, 1998 (Paper 31).